Bulletin of the Seismological Society of America

This copy is for distribution only by
the authors of the article and their institutions
in accordance with the Open Access Policy of the
Seismological Society of America.

For more information see the publications section
of the SSA website at www.seismosoc.org

THE SEISMOLOGICAL SOCIETY OF AMERICA
400 Evelyn Ave., Suite 201
Albany, CA 94706-1375
(510) 525-5474; FAX (510) 525-7204
www.seismosoc.org

Bulletin of the Seismological Society of America, Vol. 98, No. 4, pp. 1681–1695, August 2008, doi: 10.1785/0120070145

Structure of the Eastern Seattle Fault Zone, Washington State: New Insights from Seismic Reflection Data

by Lee M. Liberty and Thomas L. Pratt

Abstract We identify and characterize the active Seattle fault zone (SFZ) east of Lake Washington with newly acquired seismic reflection data. Our results focus on structures observed in the upper 1 km below the cities of Bellevue, Sammamish, Newcastle, and Fall City, Washington. The SFZ appears as a broad zone of faulting and folding at the southern boundary of the Seattle basin and north edge of the Seattle uplift. We interpret the Seattle fault as a thrust fault that accommodates north–south shortening by forming a fault-propagation fold with a forelimb breakthrough. The blind tip of the main fault forms a synclinal growth fold (deformation front) that extends at least 8 km east of Vasa Park (west side of Lake Sammamish) and defines the south edge of the Seattle basin. South of the deformation front is the forelimb breakthrough fault, which was exposed in a trench at Vasa Park. The Newcastle Hills anticline, a broad anticline forming the north part of the Seattle uplift east of Lake Washington, is interpreted to lie between the main blind strand of the Seattle fault and a backthrust. Our profiles, on the northern limb of this anticline, consistently image north-dipping strata. A structural model for the SFZ east of Lake Washington is consistent with about 8 km of slip on the upper part of the Seattle fault, but the amount of motion is only loosely constrained.

Introduction

The Seattle fault is considered the most hazardous crustal fault in the U.S. Pacific Northwest because it is located beneath the largest cities in the region and has hosted a large Holocene earthquake (Fig. 1). Uplifted terraces, tsunami deposits, and landslides show that the >70-km-long thrust or reverse fault hosted an M 7 or greater earthquake in about A.D. 900–930 (Atwater and Moore, 1992; Bucknam *et al.*, 1992; Jacoby *et al.*, 1992). The Seattle fault is more appropriately called the Seattle fault zone (SFZ) because it manifests itself as a 5–7-km-wide zone in which geologic, topographic, and geophysical data show deformed shallow strata and several fault strands (Yount and Gower, 1991; Johnson *et al.*, 1994, 1999; Pratt *et al.*, 1997; Blakely *et al.*, 2002; Nelson *et al.*, 2002; Sherrod, 2002; ten Brink *et al.*, 2002; Nelson, Johnson, Kelsey, Sherrod, *et al.*, 2003; Nelson, Johnson, Kelsey, Wells, *et al.*, 2003; Brocher *et al.*, 2004; ten Brink *et al.*, 2006).

The subsurface structure and length of the SFZ remain elusive despite extensive study. Subsurface features are known primarily from marine seismic profiles acquired in the Puget Sound and Lake Washington (Johnson *et al.*, 1999; Calvert *et al.*, 2001, 2003; ten Brink *et al.*, 2002; Fisher *et al.*, 2006). These profiles have imaged a synclinal axial surface (deformation front) that forms the south edge of the Seattle basin north of several fault strands (Pratt *et al.*, 1997; Johnson *et al.*, 1999; Nelson *et al.*, 2002; Sherrod, 2002; Nelson, Johnson, Kelsey, Sherrod, *et al.*, 2003; Nelson, Johnson, Kelsey, Wells, *et al.*, 2003). The faults themselves have not been well located from seismic profiles because they are steeply dipping and are interpreted to lie within zones of little or no reflectivity. Correlating seismic reflection discontinuities with surface exposures (Sherrod *et al.*, 2000; Nelson, Johnson, Kelsey, Sherrod, *et al.*, 2003), paleoseismic trenches (Sherrod, 2002), and light distance and ranging (lidar) topographic data (Haugerud *et al.*, 2003) also has been difficult because the marine profiles were acquired in deep troughs where the late Quaternary strata have been scoured during the most recent Quaternary glaciation (Booth, 1994).

The eastern extent of the SFZ is poorly constrained because marine waterways are absent and previous land-based seismic surveys were limited. However, a prominent magnetic lineation (anomaly A in Fig. 2b) delineates the north-dipping strata in the southern limb of a monoclinal fold at the south edge of the Seattle basin (Johnson *et al.*, 1999; Blakely *et al.*, 2002). This anomaly extends into the eastern part of the Seattle basin (Fig. 2b; Blakely *et al.*, 2002), but it broadens considerably and has not been directly correlated

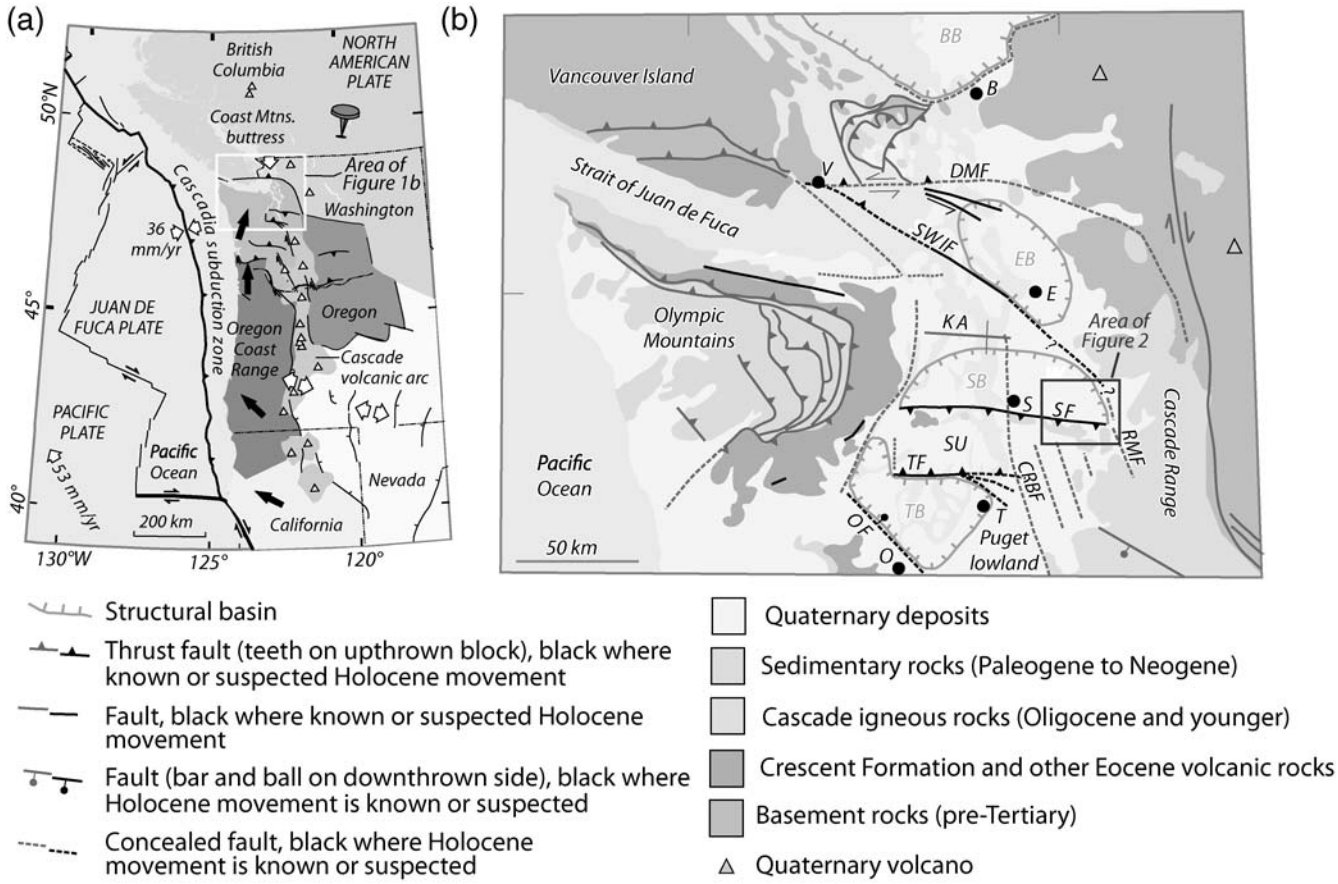

Figure 1. (a) Kinematic map of the Cascadia region or northwestern United States showing the study area at the north end of the northward-moving Coast Range block (from Wells *et al.*, 1998). (b) Map of the Puget Lowland showing major faults and exposures of basement rocks. B is Bellingham; V is Victoria; S is Seattle; T is Tacoma; O is Olympia; BB is the Bellingham basin; EB is the Everett basin; SB is the Seattle basin; TB is the Tacoma basin. DMF is the Devil's Mountain fault; SWIF is the southern Whidbey Island fault; SF is the Seattle fault; TF is the Tacoma fault; CRBF is the Coast Range Boundary fault; OF is the Olympia fault; RMF is the Rattlesnake Mountain fault; KA is the Kingston Arch; SU is the Seattle uplift. Redrawn from Brocher *et al.* (2001).

with faults or subsurface features east of Lake Sammamish. The uncertainty in the SFZ character and extent east of Lake Washington leads to uncertain estimates of maximum earthquake magnitudes. The interaction of the east part of the SFZ with other structures such as the southern Whidbey Island fault also is unknown (Fig. 1; Johnson *et al.*, 1996; Sherrod *et al.*, 2008).

We collected a series of land seismic reflection profiles to characterize the shallow (< 1 km) portions of the eastern SFZ as part of a multiyear seismic study of active faults in the Puget Lowland. Profiles were collected in the cities of Bellevue, Sammamish, and Fall City, Washington, and near a key paleoseismic trench located in Vasa Park in Bellevue (Sherrod, 2002). In addition, we incorporated published marine seismic reflection profiles from Lake Washington (Johnson *et al.*, 1999), as well as others that have not previously been interpreted (Harding *et al.*, 1988). This collection of seismic profiles shows the details of the structures within the SFZ and its hanging wall, and it further documents the SFZ's extent east of Lake Sammamish. We construct an interpretive cross section of the eastern SFZ that is consistent with these new observations east of Lake Washington.

Geologic Background

The Puget Lowland of Washington State is a broad valley between the Olympic Mountains Coast Range and the Cascade Range volcanic arc (Fig. 1). The valley is home to more than 3 million people, including the populations of Seattle, Bellevue, Tacoma, Everett, and Olympia. The Lowland lies above the Eocene suture zone between Crescent Terrane volcanic rocks and Tertiary North American crust (Johnson, 1984; Johnson *et al.*, 1996). Today, oblique convergence along the continental margin is accommodated in part by north–south shortening within the Lowland (Pratt *et al.*, 1997; Wells *et al.*, 1998; Miller *et al.*, 2001; Mazzotti *et al.*, 2002; Van Wagoner *et al.*, 2002). This shortening expresses itself as a series of basins and uplifts separated by the southern Whidbey Island, Seattle, Tacoma, and Olympia faults (Fig. 1).

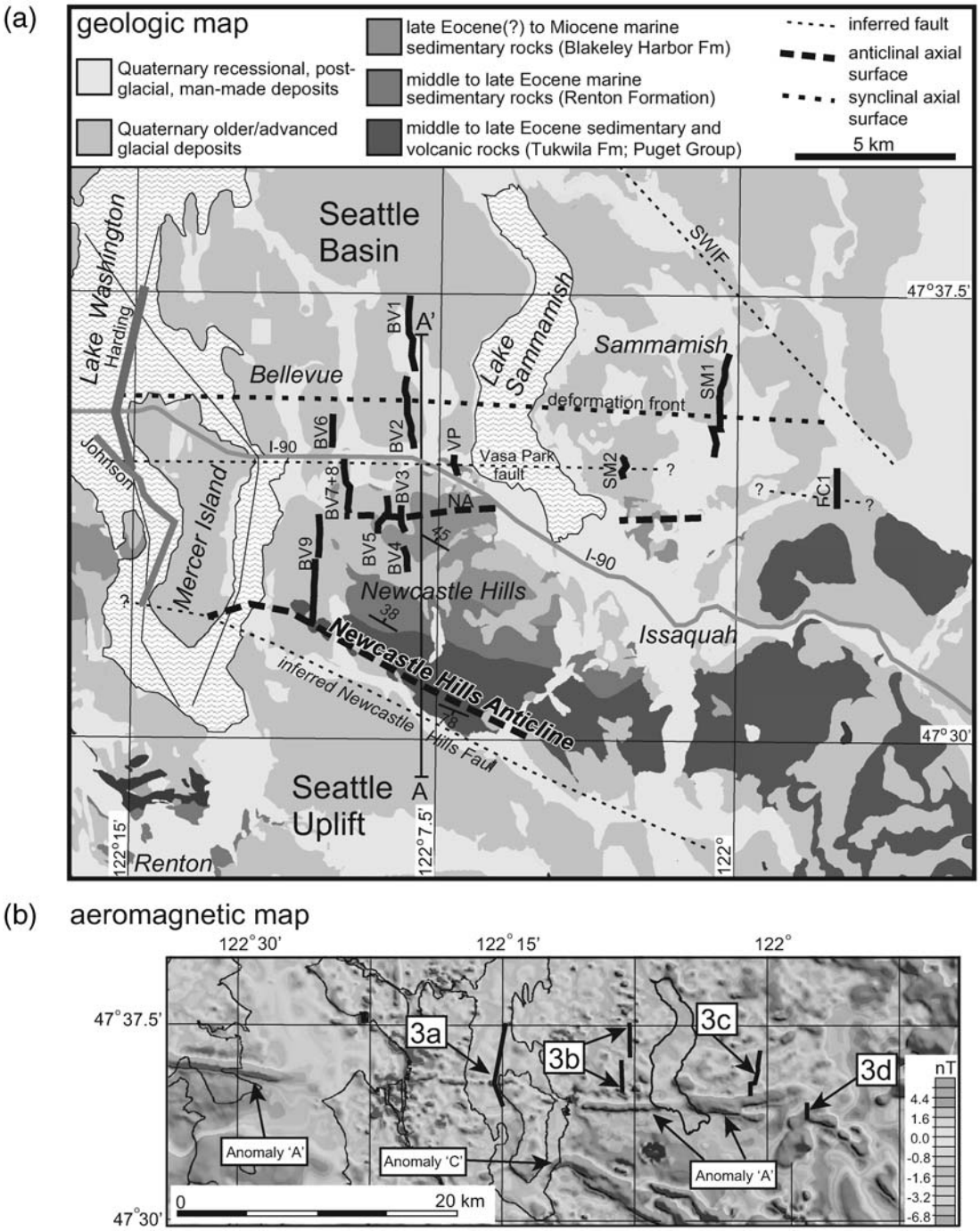

Figure 2. (a) Geologic map of the Bellevue and Sammamish area of the Puget Lowland showing the locations of the land and marine seismic reflection profiles. *A-A′* is the location of the cross section shown in Figure 6. Seismic profiles are heavy black lines with profile names next to them. VP marks the location of profiles VP1 and VP2, with the Vasa Park trench located where the profile intersects the fault. NA is the Newport anticline; I-90 is Interstate highway 90. (b) Filtered aeromagnetic anomaly map from Blakely *et al.* (2002) showing locations of seismic lines corresponding figure numbers. Anomaly *A* is interpreted to be from a dipping conglomerate layer; anomaly *C* is interpreted to be from late Eocene or Oligocene rocks in the crest of the Newcastle Hills anticline.

Of the faults beneath the Puget Lowland, the Seattle fault has the greatest vertical relief on bedrock. The fault is a north-verging thrust or reverse fault separating the approximately 8-km-thick Seattle basin on the north from uplifted basement rocks in the Seattle uplift to its south (Johnson *et al.*, 1994; Pratt *et al.*, 1997). Two recent models have been proposed for the Seattle fault: a simple thrust fault dipping to the south at ~40° with multiple strands and backthrusts at its tip (Pratt *et al.*, 1997; ten Brink *et al.*, 2002; Fisher *et al.* 2006) and a passive-roof duplex in which a shal-

low detachment separates the deeper thrust fault from the shallow fault strands (Brocher *et al.*, 2004).

Multiple late Quaternary earthquakes have been documented on the Seattle fault, including an $M > 7$ earthquake at about A.D. 900–930 (Atwater and Moore, 1992; Bucknam *et al.*, 1992; Jacoby *et al.*, 1992). This earthquake history has been discerned west of Puget Sound by the trenching of fault scarps discovered from recent lidar imagery (Sherrod *et al.*, 2000; Haugerud *et al.*, 2003; Nelson, Johnson, Kelsey, Sherrod, *et al.*, 2003; Nelson, Johnson, Kelsey, Wells, *et al.*, 2003). East of Puget Sound, the Vasa Park trench just west of Lake Sammamish (Fig. 2a) has provided crucial evidence about the eastern portion of the Seattle fault (Sherrod, 2002). The trench lies at the base of a north-facing scarp and shows clear thrusting of older strata from the south onto a paleosoil dated at 11500 ± 40 radiocarbon years B.P. (Sherrod, 2002). We refer to this strand of the SFZ as the Vasa Park fault, and it is closely associated with a magnetic lineament east of Lake Washington (anomaly *A* in Fig. 2b). Thrust motion on the Vasa Park fault is consistent with long-term motion on the SFZ but is opposite in direction to the south-vergent thrusting found in trenches west of Puget Sound (Nelson, Johnson, Kelsey, Sherrod, *et al.*, 2003; Nelson, Johnson, Kelsey, Wells, *et al.*, 2003). Although Johnson *et al.* (1999) proposed that the Seattle fault is segmented beneath Puget Sound, the A.D. 900–930 earthquake ruptured the fault on both sides of the sound (Bucknam *et al.*, 1992). Rupture east of Lake Sammamish during the A.D. 900–930 event has not been documented.

Interpretations of the shallow structure in the SFZ from seismic reflection profiles are presented by Johnson *et al.* (1999) for both west and east of Puget Sound, and ten Brink *et al.* (2002, 2006) for beneath the Puget Sound. Johnson *et al.* (1999) identify a prominent reflector within the Seattle basin as an unconformity between the Tertiary and Quaternary sediments. They place the top of undeformed Tertiary strata within the Seattle basin at approximately a 500-m depth below Lake Washington. Quaternary and Tertiary reflectors are synclinally folded at the SFZ along the south edge of the Seattle basin so that strata south of this deformation front dip to the north in a structure termed the Seattle monocline (Johnson *et al.*, 1999).

The hanging wall of the Seattle fault east of Lake Washington comprises late Eocene, Oligocene, and Miocene marine and volcaniclastic sedimentary strata that are believed to be thrust over Seattle basin sediments (Yount and Gower, 1991; Booth and Minard, 1992; Johnson *et al.*, 1994; Pratt *et al.*, 1997; Booth *et al.*, 2004; Booth *et al.*, 2008). Parallel Eocene and lower Oligocene strata in the hanging wall and Seattle basin constrain the onset of Seattle fault deformation as Oligocene or later (Johnson *et al.*, 1994; ten Brink *et al.*, 2002). A prominent anticline beneath the Newcastle Hills is cored by upper Eocene sedimentary rocks (Fig. 2a), and another magnetic anomaly (anomaly *C* in Fig. 2b) coincides with the crest of this anticline. Within the Newcastle Hills anticline, strata in the broader northern limb dip about 40°–50° north, and strata in the southern limb dip steeply to the south and are overturned in places (Yount and Gower, 1991; Booth and Minard, 1992). The anticline is bounded on the south by a prominent topographic scarp that is believed to be formed in part by a fault we term the Newcastle Hills fault (Walsh, 1984; Booth and Minard, 1992). The Newcastle Hills fault may be equivalent to the Orchard Point fault 25 km to the west, but the correlation is tenuous (Blakely *et al.*, 2002). Anticlines similar to the Newcastle Hills anticline extend across the Puget Sound south of the Seattle fault zone (Pratt *et al.*, 1997) and form the Green Mountain west of Puget Sound (Haeussler and Clark, 2000). Aeromagnetic data suggest that the SFZ continues about 7 km east of Lake Sammamish (Fig. 2b; Blakely *et al.*, 2002), but surface deformation has yet to be identified east of the lake.

Seismic Reflection Data

Land Profiles

We acquired approximately 20 km of land seismic reflection profiles with vibroseis and weight-drop sources in 14 north–south segments within the cities of Bellevue, Newport, Sammamish, and Fall City. Acquisition was constrained by major highways and other cultural features that limited the profiles to short segments (Fig. 2a). Profile segments began on the Seattle basin about 5 km north of the Vasa Park fault and extended south across the Miocene and Oligocene sedimentary rocks of the Newcastle Hills anticline. Profiles east of Lake Sammamish crossed the location of the deformation front predicted from the aeromagnetic anomalies.

We collected data primarily on quiet residential streets using a 5455-kg Industrial Vehicles International (IVI) mini-vib II vibroseis truck. We swept with a 12-sec, 20–160-Hz linear upsweep and recorded 14 sec of data to give a 2-sec record length after vibroseis correlation. The data were recorded on a 120-channel, 24-bit Geometrics RX system. We acquired the data using an offend receiver spread with 5-m source and receiver intervals to produce nominal 60-fold data with offsets up to 600 m. The shortest profiles used a fixed geophone spread with source points acquired through the spread. We recorded uncorrelated individual field records to allow precorrelation processing to attenuate the cultural noise that often plagues urban seismic surveys. Three profile segments (VP1, VP2, and FC-1) were acquired with a 200-kg, trailer-mounted, accelerated weight drop.

Vibroseis data processing included precorrelation band-pass and notch filters, and gains to minimize the effects of traffic noise and attenuate electrical noise at 60, 120, and 180 Hz. Processing of the weight-drop and postcorrelation vibroseis data included geometry, band-pass filter, multiple iterations of velocity analysis, dip moveout, common midpoint sort, ground roll and refraction mutes, automatic gain control, and stack (Yilmaz, 2001). Signal penetration ranged from more than 1.3 sec (approximately 1000 m in depth) within the Seattle basin to less than 0.4 sec (approximately

500 m in depth) on the Tertiary sediments of the Seattle uplift. Data were migrated using a phase-shift algorithm (Gazdag, 1978).

Geologic and tectonic interpretations of our data are constrained also by earlier seismic reflection profiles (e.g., Harding *et al.*, 1988; Johnson *et al.*, 1994; Pratt *et al.*, 1997; Johnson *et al.*, 1999; Calvert *et al.*, 2001, 2003; ten Brink *et al.*, 2002), regional sonic and density logs (Brocher and Ruebel, 1998), geologic maps (Yount and Gower, 1991; Booth and Minard, 1992; Pacific Northwest Center for Geologic Mapping Studies, 2006; Booth *et al.*, 2008), and aeromagnetic data (Blakely *et al.*, 2002). These earlier data, and velocity analysis of our new seismic profiles, suggest that *P*-wave seismic velocities for Pleistocene and Holocene strata average 1600–2500 m/sec when saturated and 800–1400 m/sec when unsaturated. Miocene and older sedimentary rocks within the Seattle uplift and below the Quaternary fill of the Seattle basin measure upwards of 2800 m/sec. These seismic velocities were used to convert seismic travel-time measurements to depth and to interpret strata imaged on the seismic sections.

Lake Washington Profiles

Seismic reflection data from Lake Washington (Johnson *et al.*, 1999) provide the easternmost published images from the Seattle basin and Seattle uplift before our profiles were acquired. In addition to Johnson *et al.*'s (1999) profiles, we include in our interpretation earlier profiles that were acquired but never interpreted or published in journal form (Fig. 2a; Harding *et al.*, 1988). These earlier profiles were acquired using a small (246 cm^3) airgun source and a 24-channel hydrophone streamer. Source and receiver spacing were 6.25 m, resulting in 3.125-m common-midpoint spacing. The data were largely duplicated by Johnson *et al.* (1999) using two 655-cm^3 airguns, except that Harding continued the data collection through the narrow Interstate 90 (I-90) and State Route 520 bridge openings to obtain a continuous seismic reflection profile. Unfortunately, Harding *et al.* (1988) used a Loran navigation system that resulted in large uncertainties in spatial positioning. Thus, the precise locations of the features imaged on the seismic sections are in doubt, although correlating features with Johnson *et al.*'s (1999) data can help us to more accurately locate features. Both Harding *et al.* (1988) and Johnson *et al.* (1999) also collected profiles through the narrow channel on the east side of Mercer Island. These profiles show essentially the same features as those west of the island, but the strata are not as well imaged.

We reprocessed the Harding *et al.* (1988) seismic reflection profiles from Lake Washington using dip moveout followed by a standard common-depth–point-processing sequence and a poststack frequency-wavenumber migration (Yilmaz, 2001). On the displayed profile, adjacent traces were summed for clarity giving 6.25-m common-midpoint spacing (Fig. 3a). The Johnson *et al.* (1999) data are presented here after we applied a poststack band-pass filter and migration.

Interpretation

Deformation Front

The northern part of the SFZ appears as a prominent synclinal fold, with the synclinal axial surface being the deformation front that defines the south edge of the Seattle basin (Fig. 3). Strata in the upper kilometer of the Seattle basin north of the syncline appear to be nearly flat and undeformed. The stratigraphy as imaged on the seismic data can be divided into two distinct domains that we interpret, after Johnson *et al.* (1999), as unconsolidated Quaternary deposits overlying more reflective Tertiary strata. The interpreted top of the Tertiary reflective layers is about 500 m below sea level beneath Lake Washington (Fig. 3a), about 540 m below sea level beneath Bellevue (Fig. 3b), and about 250 m below sea level beneath the city of Sammamish (Fig 3c).

Strata immediately south of the deformation front dip northward. These dipping strata comprise the Seattle monocline (Johnson *et al.*, 1999; Fig. 3). On our Bellevue and Vasa Park profiles, Tertiary strata dip at angles of up to 60° (Figs. 3b and 4). The Lake Washington profiles show Tertiary strata within the monocline dipping at angles of up to 60°, but these dips decrease northward and upward so that shallow strata near the deformation front dip less than 10° (Fig. 3a). The dips of the strata in the monocline thus decrease with decreasing age, causing the synclinal fold to sharpen downward. The monocline is consistent with growth folding, with the deeper strata being progressively rotated and the upper strata onlapping these older, more steeply dipping strata. Our interpretation is that the monocline is a growth fold above the blind tip of the northernmost strand of the Seattle fault, as suggested by Pratt *et al.* (1997) and ten Brink *et al.* (2002, 2006).

Between Lakes Washington and Sammamish, the deformation front projects to the surface about 2 km north of the topographic scarp that marks the Vasa Park fault near I-90 (Figs. 2a and 3). Beneath Lake Washington west of Mercer Island, the deformation front projects to the surface along strike about 0.5 km north of I-90 (Fig. 3a). The north-dipping strata in the monocline between the topographic scarp and the deformation front include a Miocene volcaniclastic layer that produces the prominent linear magnetic anomaly that extends from Lake Washington to Lake Sammamish (anomaly *A* in Fig. 2b; Blakely *et al.*, 2002). The continuity of the magnetic anomaly suggests that the monocline has a consistent geometry between the two lakes. Slight changes in the latitude and width of the anomalies on opposite sides of the water bodies raise the possibility that the fault is segmented by north-trending faults (e.g., Johnson *et al.*, 1999) or otherwise changes dip beneath the lakes, but our data do not resolve this question.

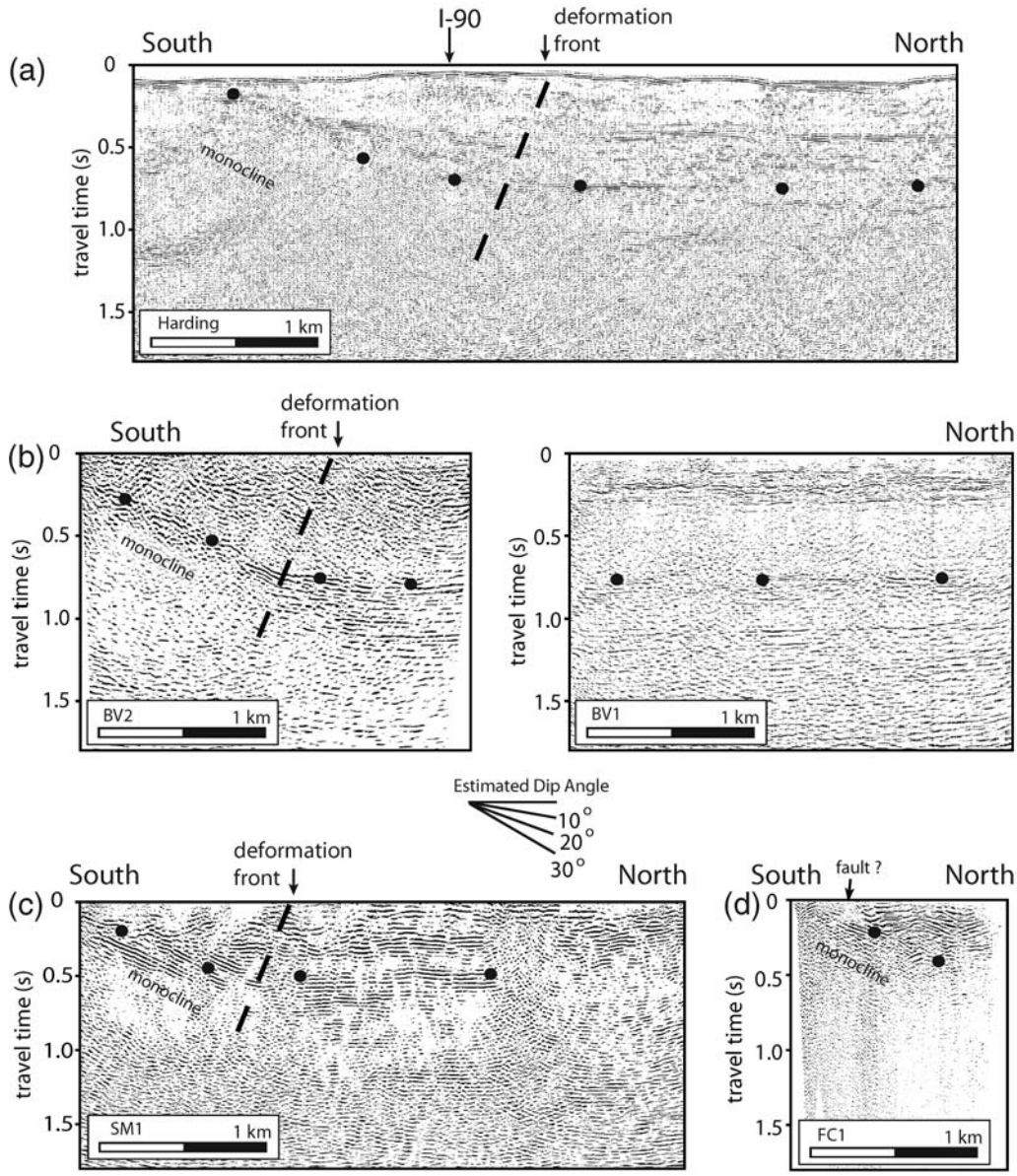

Figure 3. Seismic reflection profiles across the deformation front. (a) Harding *et al.* (1988) Lake Washington marine profile. (b) BV1 and BV2. (c) SM1. (d) FC1. Black dots show the interpreted top of Tertiary strata. Dashed lines show the synclinal axial surfaces. Vertical exaggeration is 1:1 at 2000 m/sec.

Eastern Extent of the SFZ

The deformation front extends along the SFZ with a remarkably similar geometry (Fig. 3; Johnson *et al.*, 1999; Blakely *et al.*, 2002). Using the deformation front as a proxy for the interpreted blind fault tip, we can infer a minimum eastward extent of the SFZ. Our seismic reflection profile 8 km east of Vasa Park (SM1; Fig. 3c) shows the monocline just north of the magnetic anomaly, like in the Bellevue area (Fig. 2). South of profile SM1, the magnetic anomaly forks into northern and southern strands, suggesting the intersection of two faults or a depositional change. Profile FC1 shows dipping strata (Fig. 3d) coinciding with the north edge of the southern magnetic anomaly. This magnetic anomaly and dipping strata could be delineating a southern strand of the Seattle fault, or they could be related to a second fault or fold that merges with the Seattle fault. In either case, profile FC1 suggests that faulting within the Seattle broad fault zone deforms strata as much as 11 km east of Vasa Park.

The dip of strata in the monocline appears to flatten eastward, consistent with decreasing displacement on the Seattle fault near the east edge of the Seattle basin. A distinct broadening and slight change in orientation of magnetic anomaly *A*, which is caused by a Miocene conglomerate layer, suggests flattening of Miocene stratal dips or the presence of a thicker section of Miocene rock in the east (Fig. 2b; Blakely *et al.*, 2002). The apparent dip on the top of interpreted Tertiary strata within the monocline is about 26° on all of our

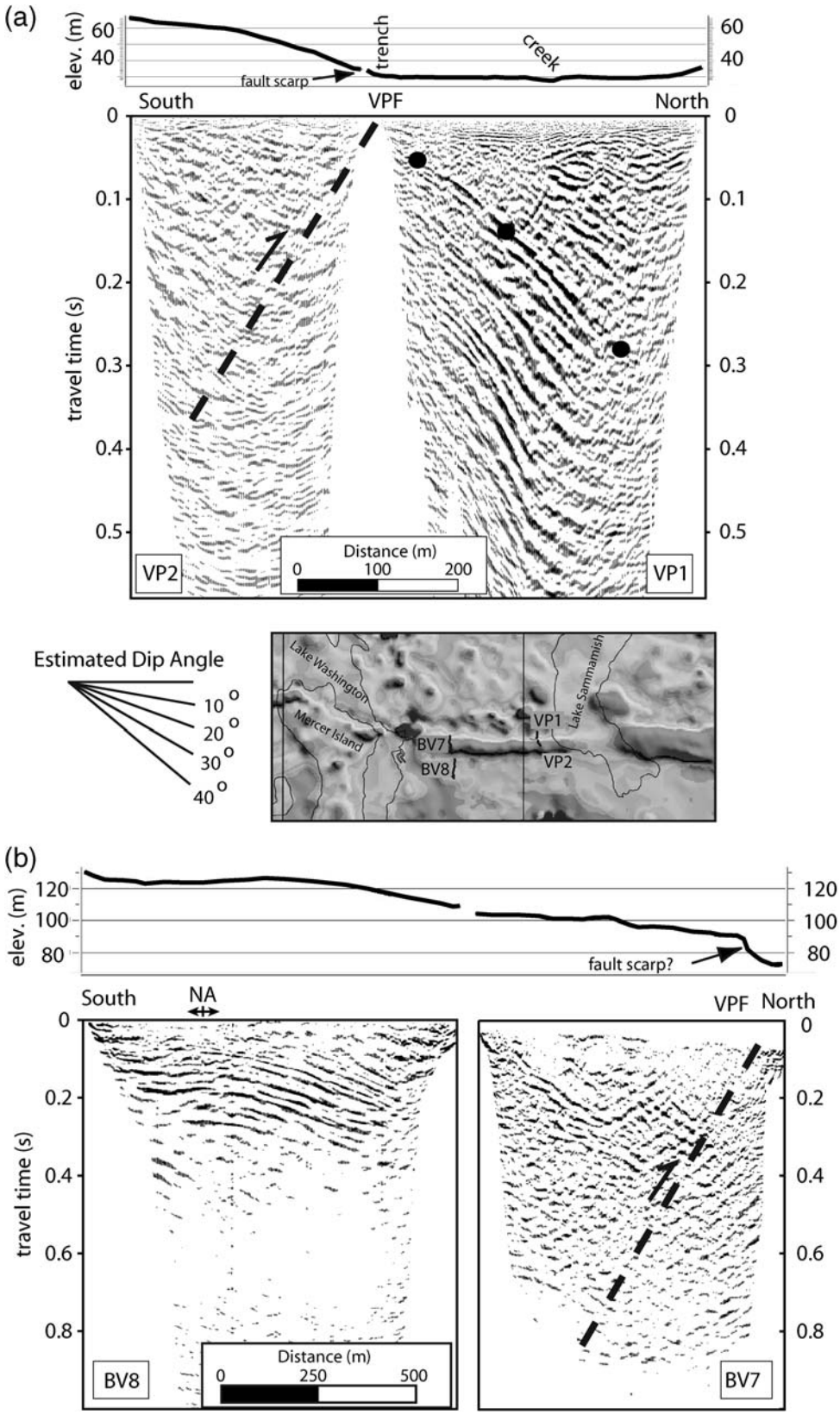

Figure 4. (a) Seismic reflection profiles VP1 and VP2 across the exposed strand of the Seattle fault in the Vasa Park trench, with the topographic profile plotted above them. (b) Profiles BV7 and BV8 across the fault at a location about 3.5 km west of the trench, with the topographic profile plotted above them. Both sets of profiles are consistent with the Vasa Park thrust or reverse fault dipping to the south at an angle of 55° or greater (dashed lines). Filtered aeromagnetic anomaly map is plotted between the sets of profiles (see Fig. 2b). Black dots show interpreted top of Tertiary strata. Vertical exaggeration is 1:1 at 2000 m/sec; VPF is the Vasa Park fault.

profiles (Fig. 3). However, these dipping strata may be of different ages. Profile SM1 lies immediately north of the magnetic anomaly (Fig. 2b), suggesting that the strata dipping at 26° on the profile are the magnetic Miocene volcaniclastic layer itself (Blakely *et al.*, 2002). In contrast, the south end of profile BV2 lies about 1 km north of the magnetic anomaly, so the reflectors dipping at 26° on that profile may be younger Miocene strata. Profile VP1, which lies in a position comparable to SM1 immediately north of the magnetic anomaly, shows presumably similar aged Miocene strata dipping at closer to 40° (Fig. 4). The Lake Washington data are more difficult to compare because of weak imaging of the steeply dipping strata and because the magnetic anomalies may be influenced by the I-90 bridge (R. Blakely, personal comm., 2007). However, the Johnson *et al.* profile (Fig. 5) shows steeply dipping (> 55°) Tertiary rock nearing the surface about 1.5 km south of the I-90 bridge, which is just north of where a magnetic anomaly is located. Thus, the profiles east of Lake Washington are consistent with strata related to the magnetic anomaly decreasing in dip toward the east edge of the basin. Eastward flattening of the monocline dips may indicate that the fault displacement decreases as the sedimentary basin thins (Snelson *et al.*, 2007). Additional complexities along the eastern edge of the Seattle basin include a change in strike of Tertiary bedrock (Walsh, 1984) and intersection with the southern Whidbey Island fault zone, which may control the northeast boundary of the Seattle basin (Fig 2a; Johnson *et al.*, 1996; Sherrod *et al.*, 2008). We thus infer that deformation associated with the SFZ extends at least 8 km east of Vasa Park as suggested from magnetic data and profile SM1, and it extends perhaps an additional 3 km east when including profile FC1. Although the dip of the bedding decreases toward the eastern edge of the Seattle basin, deformation on Tertiary and younger strata persists to the projected intersection of the southern Whidbey Island fault.

Vasa Park Fault

Our seismic reflection profiles across the topographic scarp that parallels I-90 east of Lake Washington are consistent with the exposed fault in the Vasa Park trench being either a south-dipping thrust fault or a near-vertical reverse fault. Profiles VP-1 and VP-2 cross the topographic scarp near the Vasa Park trench site (Sherrod, 2002), and profiles BV7 and BV8 extend south of I-90 approximately 3.5 km west of the trench (Fig. 2a). Late Quaternary sediments are exposed north of the trench and topographic scarp, and Miocene and older sedimentary rocks crop out to the south (Yount and Gower, 1991; Booth *et al.*, 2008). Profiles VP1 and VP2 are two short seismic profiles laterally offset due to a busy road and the steep topographic scarp, with the trench lying immediately south of the road (Fig. 4). VP1 lies on the footwall of the Vasa Park fault and VP2 is located on the hanging-wall side of the fault. Data quality on profile VP2 is diminished due to the steep topography and complex geologic conditions.

Profiles VP1, VP2, BV7, and BV8 show predominantly north-dipping strata that may be broken south of the topographic scarp by a south-dipping fault (Fig. 4). Parallel, nearly planar strata dip ~40° north in the deeper portions of profile VP1. Miocene strata are exposed for about 0.6 km south of the trench (Yount and Gower, 1991; Booth and Minard, 1992; Booth *et al.*, 2008), and we interpret the north-dipping reflectors imaged on profile VP1 as Miocene strata. Shallow, north-dipping reflectors are weak but continuous on the south half of profile VP2, but do not extend to the north side of the profile. Breaks in the reflectors are consistent with the Vasa Park fault dipping to the south at an angle of 55° or more and reaching the surface at the trench location (dashed line in Fig. 4). The continuous and unbroken reflectors imaged on profile VP1 preclude an interpretation of a north-dipping fault unless it follows a bedding plane. A north-dipping fault, however, would have to reverse its vergence in the shallow strata or have normal motion to form the south-dipping thrust fault excavated in the trench (Sherrod, 2002). We cannot eliminate the possibility of a near-vertical fault directly beneath the trench, but we favor a thrust-fault interpretation that is consistent with the overall thrust geometry of the Seattle fault discerned from regional seismic reflection profiles (Pratt *et al.*, 1997; ten Brink *et al.*, 2002; Fisher *et al.*, 2006).

We interpret the shallow, subhorizontal reflectors in the upper 30 m (0.05 sec twtt) of profile VP1 as Late Pleistocene and Holocene marine and nonmarine strata that were deposited on an uneven surface and may have been deformed subsequently by folding of the deformation front or by landslides (Fig. 4; Booth *et al.*, 2008). The uneven shallow strata coincide with a small creek that runs parallel to and 200 m north of the topographic scarp. The underlying, north-dipping strata (Miocene) are continuous beneath this disrupted area, suggesting that if faulting has disrupted the shallow strata, it must be associated with south-directed bedding-plane reverse faults associated with the folding and tilting of the deeper strata.

Profile BV7 crosses a prominent 20-m-high topographic slope that may delineate the westward extension of the Vasa Park fault immediately south of I-90 (Figs. 2 and 4). South of BV7, profile BV8 shows predominantly north-dipping Tertiary strata that appear to flatten at the crest of an anticline near the south end of the profile. These strata appear to continue beneath the south side of profile BV7, but their reflections are weaker. Like profile VP2, the north-dipping reflectors do not continue beneath the north side of profile BV7, and a series of reflector truncations are consistent with a fault that dips to the south at an angle of 55° or more from the base of the topographic scarp (dashed line in Fig. 4). As with profiles VP1 and VP2, we cannot eliminate the possibility of a near-vertical fault (dashed line in Fig. 4). Strata are not as well imaged on profile BV7 as on BV8, similar to the difference in data quality of VP2 compared to VP1. The region for a few hundred meters south of the Vasa Park fault

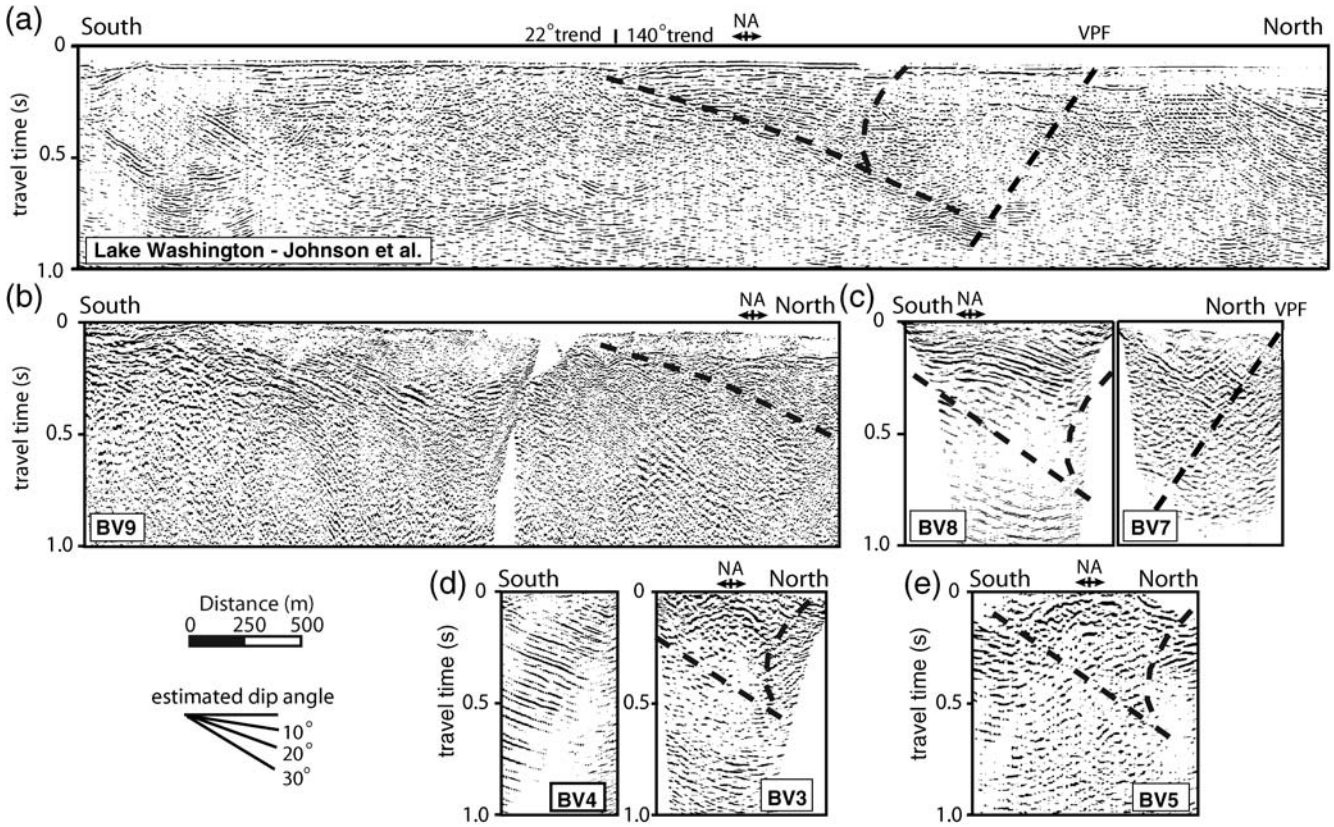

Figure 5. Seismic reflection profiles across the Newcastle Hills anticline (Fig. 2). Profiles are (a) the Lake Washington marine profile from Johnson *et al.* (1999), (b) profile BV9, (c) BV8 and BV7, (d) BV4 and BV3, and (e) BV5. All of the profiles show mostly north-dipping bedding cut by reverse faults (dashed lines). NA is the Newport anticline (see text); VPF is the Vasa Park fault. Vertical exaggeration is 1:1 at 2000 m/sec.

may be a region of deformed strata in which fractures and folds decrease the reflector continuity.

The location of the Vasa Park fault on the Lake Washington profile is ambiguous if it extends that far west. Projecting the Vasa Park fault to the west, our estimate is that the fault lies in a relatively nonreflective part of the profile between two zones of north-dipping reflectors, similar to the reflector geometry observed on the Vasa Park and BV7/8 profiles (Fig. 5a). Again, we do not see clear evidence of the fault at this location, but continuous, north-dipping reflectors make faults unlikely in the regions immediately north and south of this nonreflective zone.

The dipping strata in the footwall immediately north of the Vasa Park fault on VP1 (Fig. 4) provide important constraints on the structure and amount of slip on the SFZ. Because the dips of the strata in the footwall and hanging wall of the Vasa Park fault are both similar to those in the northern limb of the Newcastle Hills anticline, they all must have been folded together above a deeper fault before being cut by the Vasa Park fault. This deeper fault must be the main splay of the Seattle fault (the strand with the greatest displacement), because it tilts a large volume of strata to angles of 40°–50°, whereas the Vasa Park fault does not appear to produce a large change in stratal dips. One potential model is that the north-dipping strata are part of the forelimb of a fault-propagation fold above the deeper fault, with the trench fault being a forelimb breakthrough (Fig. 6; Suppe and Medwedeff, 1990).

The age of the strata in the footwall of the Vasa Park fault, which is currently unknown, could provide an important constraint on the amount of displacement on the Vasa Park fault. If the footwall strata are significantly younger than the hanging-wall strata, it implies a substantial amount of displacement, but if the strata are nearly the same age, it implies a relatively small amount of displacement. However, the exposures of 9–15 Ma strata in the hanging wall just south of the trench site (Booth *et al.*, 2008), combined with the similar dips of footwall and hanging-wall strata of the Vasa Park fault, limits the total Miocene and younger displacement on the fault to being less than the thickness of the Miocene strata in the area (Fig. 6). Greater displacements would have removed all of the Miocene strata from the hanging wall or would require a significant change in stratal dip across the fault zone. Although regionally the Miocene strata may reach as much as ~3 km in thickness (Fulmer, 1975; McLean, 1977; Johnson *et al.*, 1994; Pratt *et al.*, 1997; ten Brink *et al.*, 2002), their thickness where exposed near Vasa Park is likely nearer 0.5 km (Booth and Minard, 1992; Booth

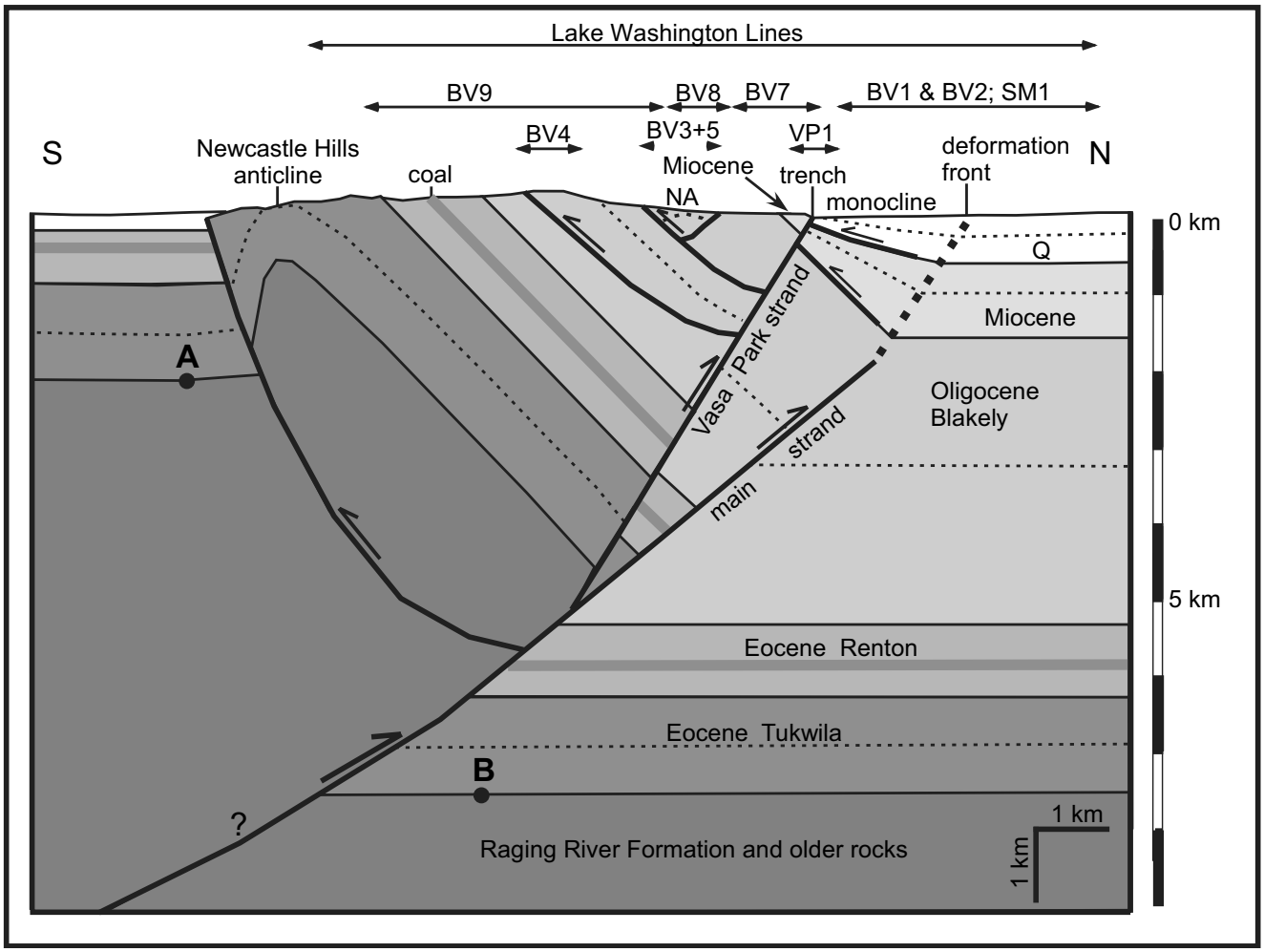

Figure 6. Interpretive north–south cross section through Bellevue (see Fig. 2 for location). The cross section shows the Seattle fault as a fault-propagation fold with a forelimb breakthrough and a backthrust. Points *A* and *B* show the estimated depths to basement rocks, with a total of about 5 km of vertical displacement. See text for explanation. NA is the Newport anticline.

et al., 2008). Post-Miocene displacement on the Vasa Park strand of the SFZ thus is likely less than about 0.5 km.

Newcastle Hills Anticline

The area south of the SFZ between Lakes Washington and Sammamish is underlain by the Newcastle Hills anticline, which has strata on its northern limb dipping 35°–50° north and strata on its southern limb dipping at about 70°–80° south (Walsh, 1984; Yount and Gower, 1991; Pacific Northwest Center for Geologic Mapping Studies, 2006). A prominent magnetic lineament (anomaly *C* in Fig. 2b; Blakely *et al.*, 2002) correlates with Tukwila formation rocks that reach shallow depths in the axis of the anticline. Seismic profiling in the Puget Sound (Pratt *et al.*, 1997) and geologic mapping farther west (Haeussler and Clark, 2000) suggest that similar anticlines in and south of the SFZ continue west to Green Mountain near Bremerton (Blakely *et al.*, 2002). Our seismic reflection profiles south of I-90 all lie on the north flank of the Newcastle Hills anticline, with profile BV9 just nearing its crest (Fig. 2). The crest of the anticline may not be crossed by the Lake Washington profiles west of Mercer Island, as the rocks causing the magnetic anomaly appear to bend to the south and to be truncated by the extension of the inferred Newcastle Hills fault (Fig. 2a).

All of our land seismic reflection profiles south of I-90 show predominantly north-dipping parallel strata within the northern limb of the anticline (Fig. 5). Profiles BV4 and BV9, along with both Lake Washington profiles, all show north-dipping, nearly planar reflectors dipping to the north at angles from 20°–40°. Profile BV4 lies about 1 km north of the coal seams that were extensively mined in the late 1800s and early 1900s near the center of the Renton formation (Walsh, 1983). These coal seams are remarkably planar and dip north at 35°–45°. They extend unbroken for nearly 8 km along the northern limb of the Newcastle Hills anticline from just east of our profile BV9 to south of Lake Sammamish, where the trend changes slightly (~20°) northward about 1 km west of Issaquah (Walsh, 1983). The coal seams also

are present southeast of Lake Sammamish, with the valley south of the lake interrupting the otherwise continuous seams. The downdip extensions of the coal seams presumably lie 300–500 m below the deepest reflectors visible on profile BV4. The continuity and planar attitude of these coal seams is important evidence that much of the Newcastle Hills anticline is not disrupted by faults or deformed except by the broad folding. The exception is that the coal seams are not known beneath the location of our profile BV9, which may indicate that a north–south fault or fold lies in the north-trending valley between our profiles BV8 and BV9.

One notable exception to the north-dipping strata in the northern limb of the Newcastle Hills anticline is a small anticline with an axis parallel to the SFZ (Fig. 2a) that we term the Newport anticline. Profiles BV3 and BV5 show the Newport anticline as arched reflectors, about 1 km across, above zones of convergent reflectors marking faults (Fig. 5). The northern side of the Newport anticline is also apparent on profile BV8, where it is broader and the reflectors have gentler dips. The anticline is mapped for 3 km east of profile BV3 to Lake Sammamish, and possibly for several kilometers east of Lake Sammamish (Fig. 2a; Yount and Gower, 1991). It may also extend to Lake Washington, where the Johnson *et al.* (1999) profile shows what appears to be arched reflectors above the north-dipping strata (Fig. 5). The anticline is nearly parallel to the deformation front, suggesting that it is a component of the SFZ. Possible interpretations are that the anticline is the surface expression of a small backthrust (Fig. 6; e.g., ten Brink *et al.*, 2002), or that the anticline is formed by a strike-slip fault cutting the hanging wall.

Another small anticline or disrupted zone also may be imaged on profile BV9 about 1 km south of the Newport anticline (Fig. 5). North-dipping strata appear to roll over or terminate upward, with an unconformity above. This structure is south of our other land profiles except BV4, on which it is not apparent. Yount and Gower (1991) show a southwest-trending fault approximately in this area, but the fault does not appear on subsequent maps by Booth and Minard (1992) and Booth *et al.* (2008). If not fault related, the structure imaged on the seismic profiles could be an erosional unconformity at the upward truncation of north-dipping reflectors.

Structural Model of the Eastern SFZ

Figure 6 shows our hypothesized cross section of the SFZ and Newcastle Hills anticline based on geologic data and the seismic reflection profiles. The following observations were satisfied when constructing this cross section.

1. The deformation front is a synclinal axial surface about 2 km in front of the Vasa Park fault exposed in the trench, with Quaternary growth faulting demonstrated by onlapping strata and increasing stratal dip with increasing depth (Fig. 3a; Johnson *et al.*, 1999).
2. The Vasa Park trench exposed the south-dipping Vasa Park thrust fault at the surface, the seismic profiles are consistent with a south-dipping thrust or reverse fault at the trench, and the topographic scarp indicates the south-side-up motion on that strand of the Seattle fault zone (Sherrod, 2002).
3. Strata in both the hanging wall and footwall of the Vasa Park fault dip to the south with a common dip of 35°–50°, suggesting that the fault cut through a section of strata that were already tilted above the deeper main strand of the fault.
4. There are Miocene rocks exposed in the hanging wall of the Vasa Park fault just south of the trench (Booth *et al.*, 2008), which implies that motion on the fault strand is less than the thickness of the Miocene strata. The thickness of Miocene strata is unknown in this area, but is likely about 0.5 km where mapped in the monocline.
5. A fault with north-side-up motion bounds the south side of the Newcastle Hills anticline, which has steeply south-dipping or overturned beds on its south edge near the hypothesized fault (Walsh, 1984; Yount and Gower, 1991; Booth and Minard, 1992; Booth *et al.*, 2008). A prominent magnetic high (Fig. 2b; Blakely *et al.*, 2002) suggests that magnetic Tukwila formation rocks lie at the surface along the crest of the anticline.
6. Motion on the Seattle fault during the Miocene and possibly Oligocene implies that strata of these ages are growth strata that are thinner in the hanging wall than in the footwall (Johnson *et al.*, 1994; Pratt *et al.*, 1997; ten Brink *et al.*, 2002).

We favor a thrust-fault model for the SFZ in which the Seattle uplift is a large fault-propagation fold with a forelimb breakthrough (Suppe and Medwedeff, 1990; Shaw *et al.*, 2005). The Newport Hills anticline lies between the main thrust fault and a large backthrust. The deformation front is interpreted as the synclinal axial surface above the main blind fault tip. The exposed fault in the Vasa Park trench is interpreted as the forelimb breakthrough fault. In the monocline, we interpret growth folding, which creates minor bedding-plane backthrusts that disrupt the shallow strata near the Vasa Park fault (Fig. 4). Additional backthrusts occur within the northern limb of the Newcastle Hills anticline, one of which creates the small Newport anticline superimposed on its northern limb (Fig. 5). The model is effectively unconstrained south of the large backthrust at the south edge of the Newcastle Hills anticline, except that strata have been lifted substantially by motion on the main thrust fault so that Eocene rocks crop out to the south of the Lake Washington (Fig. 2).

The total displacement at the tip of the Vasa Park fault strand is limited to the thickness of the Miocene section because strata of that age lie in the hanging wall just south of the trench. However, a substantial amount of slip must be consumed by folding within the forelimb of the fault-

propagation fold and by backthrusts, so the total amount of slip on the deeper portions of the fault is substantially greater than at the fault tips.

The deeper portion of the Seattle fault is largely unconstrained by our data, except that the Vasa Park fault must intersect the main fault at depth. This requires the main fault to dip at a shallower angle than the Vasa Park fault, which may dip to the south at as little as 55°. We have drawn the main fault to an 8-km depth at about a 40° angle, which is consistent with the 40° dip estimated by ten Brink *et al.* (2002) from seismic tomography and with apparent fault-plane reflections documented by Fisher *et al.* (2006) beneath the Puget Sound. The presence of Tukwila formation at the axis of the anticline implies that Eocene basement rocks are relatively shallow in this part of the hanging wall. This in turn requires that the Seattle fault extend into the basement rocks, which now lie at a depth of at least 7 km beneath the Seattle basin. If we assume that the top of the Eocene basement rocks started as a relatively flat surface at the end of the Eocene, as seems likely given the flat bedding within the overlying Tukwila and Renton formations, the Seattle fault appears to root at a depth of more than 7 km. However, the Seattle basin is believed to have subsided as much as 3 km in response to motion on the Seattle fault (Johnson *et al.*, 1994; Pratt *et al.*, 1997; ten Brink *et al.*, 2002), which means that the top of the Crescent formation may have been at a depth closer to 4 or 5 km when motion on the Seattle fault began. Thus, the Seattle fault likely roots at a depth of at least 4 km, probably deeper.

Our model does not agree with the passive-roof duplex model (Brocher *et al.*, 2004) for two reasons. First, the presence of Eocene rocks (Tukwila formation) at the surface in the Newcastle Hills anticline would require those rocks to be transported from depths of about 4 km or more in the footwall into the hanging wall of the roof thrust—in other words, from below to above the horizontal detachment in the passive-roof duplex model. This requires that the Eocene rocks were brought near to the surface by the deeper thrust faults before the roof thrust formed, requiring much of the shortening on the deeper thrust faults to have occurred before motion on the roof thrust is initiated. Subsequent Miocene shortening within the roof thrust must be balanced by an equal amount of shortening in the underlying basement thrusts, which would further lift the basement rocks and exhume the roof thrust. Thus, there appears to be an inconsistency between the amount and timing of shortening in the roof thrust and basement thrusts in a passive-roof duplex model. Alternatively, the roof thrust has been exhumed in the Bellevue region, and we are looking at structures that lie within the footwall.

Second, the passive-roof duplex model does not explain the growth folding in the north-dipping strata at and south of the deformation front. A thrust wedge being driven between strata at the fault tip would fold all of the overlying strata within an upward-thinning growth triangle to a uniform dip angle (see Pratt *et al.* [2002] for a kinematic model of such a wedge in the Coyote segment of the Puente Hills fault). In contrast, the seismic profiles, particularly the Lake Washington profile (Fig. 3a), show an upward decrease of stratal dips and onlap of strata within the monocline. Our interpretation of the monocline as the forelimb of a fault-propagation fold would account for this geometry through growth folding and progressive limb rotation (Hardy and Poblet, 1994; Shaw *et al.*, 2005).

Discussion

Slip on the Seattle Fault

The relatively small amount of slip at the fault tips in our model in comparison to the amount of slip on deeper portions of the fault highlights an important point about the interpretation of paleoseismic data in the region: only a portion of the slip on the deeper parts of the fault reaches the surface. Slip on thrust or reverse faults often decreases updip as folding and backthrusts consume some of the slip occurring on deeper parts of the fault (e.g., Suppe and Medwedeff, 1990; Shaw *et al.*, 2005). This implies that only some of the earthquakes that occur on a fault are expressed as surface ruptures that might be visible as discreet faults in trenches, although the largest earthquakes presumably rupture a large enough fault area to reach the surface. It also implies that slip rates calculated from surface ruptures and shallow strata do not necessarily indicate the total slip present on the deeper portions of the faults.

An estimate of the total shortening on the deep part of the Seattle fault on our cross section can be made from the elevation difference in the top of Eocene basement rocks across the fault (points *A* and *B* in Fig. 6). Late Eocene rocks are exposed at several locations 4–8 km south of the Newcastle Hills anticline (Fig. 2; Yount and Gower, 1991; Pacific Northwest Center for Geologic Mapping Studies, 2006), which indicates that late Eocene rocks lie at shallow depths south of the anticline. Comparable rocks likely lie at about 5–6 km depth beneath the eastern part of the Seattle basin near our cross section (Snelson *et al.*, 2006) We estimate a vertical elevation change of about 5 km for the top of the basement rocks on opposite sides of the Seattle fault, although neither of these depths is well constrained. Assuming a fault dip of 40° implies about 8 km of motion on the deeper part of the main fault to create this vertical change. This is smaller than the ~10 km of motion interpreted by ten Brink *et al.* (2002) near the Puget Sound where the Seattle basin is deeper (Snelson *et al.*, 2006). If motion began in the Oligocene as hypothesized by Johnson *et al.* (1994) and Pratt *et al.* (1997), it implies a slip rate of at least 0.25 mm/yr over the past 32 million years. If motion began in the middle Miocene, as interpreted by ten Brink *et al.* (2002), the slip rate would be about 0.53 mm/yr over the past 15 million years. These numbers are consistent with earlier estimates of slip rate, but our estimates are only loosely constrained because

of the large uncertainties in the depths of the Eocene rocks north and south of the Newcastle Hills anticline.

We can also estimate a maximum slip rate for the Vasa Park fault by assuming that the maximum post-Miocene displacement is limited to the thickness of the Miocene strata exposed in the hanging wall above the trench. If we assume a thickness of 0.5 km for Miocene strata, the slip rate near the surface would be limited to a maximum average of about 0.07 mm/yr since late Miocene (7 Ma). If we assume the maximum thickness of 2.5 km for Miocene strata interpreted in the center of the Seattle basin (Johnson *et al.*, 1994), the slip rate could be as high as 0.35 mm/yr. The aforementioned estimates of slip rate suggest a repeat time of 5700–28,500 for earthquakes with a 2-m characteristic slip. These recurrence times are consistent with the one large postglacial event documented in the Vasa Park trench between 4500 and 10,500 yr ago (Sherrod, 2002). Long recurrence times between surface-rupturing events therefore appear to be plausible; however, substantial slip on deeper portions of the fault, and thus potentially large earthquakes, may also occur without surface rupture.

Along-Strike Variations in the Seattle Fault

Although there appears to be a difference between the Seattle fault on the east and west sides of the Puget Sound in terms of the vergence of the faults causing the latest surface ruptures, the overall fault-propagation fold structure is a viable interpretation for the Seattle fault on both sides of the Puget Sound. West of Puget Sound, the latest surface-rupturing events caused north-side-up motion, which implies that the deeper fault motion reached the surface on backthrusts (e.g., ten Brink *et al.*, 2002, 2006). However, the broad region of uplift evident along the wave-cut terrace is likely caused by motion on a buried fault tip (ten Brink *et al.*, 2006). Thus, the Seattle fault on the west side of the Puget Sound can be explained by a similar fault geometry to the one we propose here except that the forelimb breakthrough fault (the Vasa Park fault) is either absent or has not had recent motion to break the wave-cut terrace on Bainbridge Island. The seismic reflection profiles from the Puget Sound show reflector truncations that are consistent with a forelimb breakthrough fault (Pratt *et al.*, 1997).

The hypothesized backthrusts east of the Puget Sound and Lake Washington may have had surface rupture that is no longer visible because of urban development. The Newport anticline, a possible backthrust on profile BV9, and the large backthrust on the south edge of the Newcastle Hills anticline are presumably associated with folding of the anticline, but this could include Holocene deformation. These areas are now covered by urban development that makes recognition of surface ruptures difficult or impossible in lidar data or from geologic studies.

Lake Sammamish may form a north–south boundary across which the SFZ changes. East of Lake Sammamish, the strike of geologic structures in the hanging wall of the Seattle fault appears to change to a northeast trend (Yount and Gower, 1991). Likewise, the magnetic anomalies appear broader and the seismic data show shallower dips in the Seattle monocline east of the lake (Fig. 3; Blakely *et al.*, 2002). Prunier (1998) presents evidence from high-resolution seismic profiles for a north-trending fault beneath the north end of Lake Sammamish. We therefore raise the possibility that Lake Sammamish marks a segment boundary in the Seattle fault, across which the fault geometry changes slightly. If present, this segment boundary likely represents a minor tear because the basic SFZ characteristics appear to be continuous across most of the Puget Lowland (Blakely *et al.*, 2002).

Lake Washington and the valley between our profiles BV8 and BV9 also could be the locations of north–south faults in the hanging wall of the Seattle fault. The coal seams that are present east of our profile BV8 are not present in the hills beneath our profile BV9. The area between the two profiles is a deep north-trending valley that could delineate a fault. Likewise, the magnetic anomalies that are so continuous east of Lake Washington may terminate, abruptly change trend, or shift to the north on opposite sides of Mercer Island (although the influence of the I-90 bridge on the magnetic anomalies is not clear). One explanation is that Lake Washington coincides with a north-trending fault that lies beneath or on the east side of Mercer Island.

Conclusions

High-resolution land seismic reflection profiles provide new information about the SFZ east of Lake Washington. The profiles image the deformation front to at least 8 km east of Vasa Park, consistent with the eastward extent of an aeromagnetic anomaly. Deformation of Tertiary and younger strata at Fall City suggest that the Seattle fault may extend farther east. South of the deformation front, north-dipping strata in the northern limb of the Newcastle Hills anticline dominate the seismic reflection profiles. The presence of a thrust fault in the Vasa Park trench just west of Lake Sammamish indicate these north-dipping strata are cut by a thrust fault, although the fault itself is poorly imaged on the seismic profiles. The data are consistent with a fault-propagation fold model for the north-verging Seattle fault. The main elements of the model are a blind fault tip beneath the deformation front, a forelimb breakthrough (the Vasa Park fault), and a large backthrust. The Newcastle Hills anticline is formed between the main thrust fault and the large backthrust. The model is consistent with about 8 km of motion on the Seattle fault, although more motion could be present on the deeper parts of the fault.

Acknowledgments

This work was accomplished with the support of U.S. Geological Survey National Earthquake Hazards Reduction Program (NEHRP) Award Number 03HQGR0132 and by the Landmark Graphics Corporation via the Landmark University Grant Program. We thank the many volunteers

who helped us collect the seismic reflection profiles, as well as the full-time crew of Gregg Beukelman, Scott Hess, Amy Allen, and Mike Clair. We thank King County, the cities of Sammamish, Newcastle, and Bellevue, the Bellevue water district, and the Parks Departments of Sammamish and Bellevue for permission to operate on maintained grounds and roads. The manuscript benefited from reviews by William Stephenson and Kathy Troost, and from discussions with Megan Anderson, Derek Booth, Thomas Brocher, Brian Sherrod, and Timothy Walsh.

References

Atwater, B. F., and A. L. Moore (1992). A tsunami about 1000 years ago in Puget Sound, Washington, *Science* **258,** 1614–1617.

Blakely, R. J., R. E. Wells, C. S. Weaver, and S. Y. Johnson (2002). Location, structure, and seismicity of the Seattle fault, Washington, *Geol. Soc. Am. Bull.* **114,** 169–177.

Booth, D. B. (1994). Glaciofluvial infilling and scour of the Puget Lowland, Washington, during ice-sheet glaciation, *Geology* **22,** 695–698.

Booth, D. B., and J. P. Minard (1992). Geologic map of the Issaquah 7.5' quadrangle, King County, Washington, *U.S. Geol. Surv. Misc. Studies Map MF-2206*.

Booth, D. B., K. G. Troost, and J. T. Hagstrum (2004). Deformation of Quaternary strata and its relationship to crustal folds and faults, south-central Puget Lowland, Washington State, *Geology* **32,** 505–508.

Booth, D. B., T. J. Walsh, K. G. Troost, and S. A. Shimel (2008). Geologic map of the Issaquah 7.5-minute quadrangle, Washington, *U.S. Geol. Surv. Misc. Field Invest.*, scale 1:24,000 (in press).

Brocher, T. M., and A. L. Ruebel (1998). Compilation of 29 sonic and density logs from 23 oil test wells in western Washington State, *U.S. Geol. Surv. Open-File Rept. 98-249*, 1–60.

Brocher, T. M., R. J. Blakely, and R. E. Wells (2004). Interpretation of the Seattle uplift, Washington, as a passive-roof duplex, *Bull. Seismol. Soc. Am.* **94,** 1379–1401.

Brocher, T. M., T. Parsons, R. A. Blakely, N. I. Christensen, M. A. Fisher, R. E. Wells, and the SHIPS Working Group (2001). Upper crustal structure in Puget Lowland, Washington: results from 1998 seismic hazards investigation in Puget Sound, *J. Geophy. Res.* **106,** 13,541–13,564.

Bucknam, R. C., E. Hemphill-Haley, and E. B. Leopold (1992). Abrupt uplift within the past 1,700 years at southern Puget Sound, Washington, *Science* **258,** 1611–1614.

Calvert, A. J., and M. A. Fisher The SHIPS Working Group (2001). Imaging the SFZ with high-resolution seismic tomography, *Geophys. Res. Lett.* **28,** 2337–2340.

Calvert, A. J., M. A. Fisher, and S. Y. Johnson The SHIPS Working Group (2003). Along-strike variations in the shallow seismic velocity structure of the SFZ: evidence for fault segmentation beneath Puget Sound, *J. Geophys. Res.* **108,** no. B1, 2005, doi 10.1029/2001JB001703.

Fisher, M. A., R. D. Hyndman, S. Y. Johnson, T. M. Brocher, R. S. Crosson, R. E. Wells, A. J. Calvert, and U. S. ten Brink (2006). Crustal structure and earthquake hazards of the subduction zone in southwestern British Columbia and western Washington, in *Earthquake Hazards of the Pacific Northwest Costal and Marine Regions*, R. Kayen (Editor), *U.S. Geol. Surv. Profess. Pap. 1661-C,*, 28 pp.

Fulmer, C. V. (1975). Stratigraphy and paleontology of the type Blakeley and Blakely Harbor formations, in the Paleogene Symposium and Selected Technical Papers, *Conference on Future Energy Horizons of the Pacific Coast: American Association of Petroleum Geologists, Pacific Section, v. 50*, D. W. Weaver, G. R. Hornaday and Ann Tipton (Editors), Fiftieth Joint Annual Meeting of Pacific Sections of American Association of Petroleum Geologists, Society of Economic Paleontologists and Mineralogists, and Society of Exploration Geophysicists, Long Beach, California, April 23–26, 1975, p. 210–271.

Gazdag, J. (1978). Wave equation migration with the phase-shift method, *Geophysics* **43,** 1342–1351.

Haeussler, P. J., and K. P. Clark (2000). Preliminary geologic map of the Wildcat Lake 7.50 quadrangle, Kitsap and Mason Counties, Washington, *U.S. Geol. Surv. Open-File Rept. 00-356*, scale 1:24,000.

Harding, S. T., T. P. Barnhard, and T. C. Urban (1988). Preliminary data from the Puget Sound multichannel seismic-reflection survey, *U.S. Geol. Surv. Open-File Rept. 88-698*, 9 pp.

Hardy, S., and J. Poblet (1994). Geometric and numerical model of progressive limb rotation in detachment folds, *Geology* **22,** 371–374.

Haugerud, R., D. J. Harding, S. Y. Johnson, J. L. Harless, C. S. Weaver, and B. L. Sherrod (2003). High-resolution lidar topography of the Puget Lowland, Washington, *GSA Today* **13,** 4–10.

Jacoby, G. C., P. L. Williams, and B. M. Buckley (1992). Tree ring correlation between prehistoric landslides and abrupt tectonic events in Seattle, Washington, *Science* **258,** 1621–1623.

Johnson, S. Y. (1984). Evidence for a margin-truncating transcurrent fault (pre–late Eocene) in western Washington, *Geology* **12,** 538–541.

Johnson, S. Y., C. J. Potter, and J. M. Armentrout (1994). Origin and evolution of the Seattle basin and Seattle fault, *Geology* **22,** 71–74.

Johnson, S. Y., S. V. Dadisman, J. R. Childs, and W. D. Stanley (1999). Active tectonics of the Seattle fault and central Puget Lowland: implications for earthquake hazards, *Geol. Soc. Am. Bull.* **111,** 1042–1053.

Johnson, S. Y., C. J. Potter, J. M. Armentrout, J. J. Miller, C. Finn, and C. S. Weaver (1996). The southern Whidbey Island fault, an active structure in the Puget Lowland, Washington, *Geol. Soc. Am. Bull.* **108,** 334–354.

Mazotti, S., H. Dragert, and R. D. Hyndman (2002). N-S shortening across the Olympic Mountains and Puget Sound evidenced by GPS, *Geol. Soc. Am. Abstr. Programs* **34,** A90.

McLean, H. (1977). Lithofacies of the Blakeley formation, Kitsap County, Washington: a submarine fan complex, *J. Sediment. Petrol.* **47,** 78–88.

Miller, M. M., D. J. Miller, C. M. Rubin, H. Dragert, K. Wang, A. Qamar, and C. Goldfinger (2001). GPS-determination of along-strike variation in Cascadia margin kinematics: implications for relative plate motion, subduction zone coupling, and permanent deformation, *Tectonics* **20,** 161–176.

Nelson, A. R., S. Y. Johnson, H. M. Kelsey, B. L. Sherrod, R. E. Wells, K. Okumura, L.-A. Bradley, and R. Bogar (2003). Field and laboratory data form an earthquake history study of the Waterman Point fault, Kitsap County, Washington, *U.S. Geol. Surv. MF-Map 2423*, 1 plate.

Nelson, A. R., S. Y. Johnson, H. M. Kelsey, R. E. Wells, B. L. Sherrod, S. K. Pezzopane, L. Bradley, and R. D. Koehler III (2003). Late Holocene earthquakes on the Toe Jam Hill fault, SFZ, Bainbridge Island, Washington, *Geol. Soc. Am. Bull.* **115,** 1388–1403.

Nelson, A. R., S. Y. Johnson, R. E. Wells, S. K. Pezzopane, H. M. Kelsey, B. L. Sherrod, L. A. Bradley, R. D. Koehler III, R. C. Bucknam, R. A. Haugerud, and W. T. LaPrade (2002). Field and laboratory data from an earthquake history study of the Toe Jam Hill fault, Bainbridge Island, Washington, *U.S. Geol. Surv. Open-File Rept. 02-60*, 37 pp., 2 plates.

Pacific Northwest Center for Geologic Mapping Studies (2006). Geologic map of King County, Washington, Booth, D. B., and A. P. Wisher, Compilers, available at http://geomapnw.ess.washington.edu/services/publications/map/data/KingCo_composite.pdf, scale 1:100,000 (last accessed June 2008).

Pratt, T. L., S. Y. Johnson, C. J. Potter, and W. J. Stephenson (1997). Seismic reflection images beneath Puget Sound, western Washington State: the Puget Lowland thrust sheet hypothesis, *J. Geophys. Res.* **102,** 27,469–27,490.

Pratt, T. L., J. H. Shaw, J. F. Dolan, S. Christofferson, R. A. Williams, J. K. Odum, and A. Plesch (2002). Shallow seismic imaging of folds above the Puente Hills blind-thrust fault, Los Angeles, California, *Geophys. Res. Lett.* **29,** 18-1–18-4.

Prunier, C. F. (1998). Holocene faulting and landsliding in Lake Sammamish related to the Seattle fault, *Master's Thesis*, University of Nevada, Reno, Nevada.

Shaw, J. H., C. Connors, and J. Suppe (2005). *Seismic Interpretation of Contractional Fault-Related Folds: An AAPG Seismic Atlas*, American

Association of Petroleum Geologists Studies in Geology, No. 53, AAPG, Tulsa, Oklahoma, 157 pp.

Sherrod, B. L. (2002). Late Quaternary surface rupture along the Seattle fault zone near Bellevue, Washington (Abstract S21C-12), *Eos Trans. AGU* **83,** no. 47 (Fall Meet. Suppl.), S21C-12.

Sherrod, B. L., R. C. Bucknam, and E. B. Leopold (2000). Holocene relative sea level changes along the Seattle fault at Restoration Point, Washington, *Quat. Res.* **54,** 384–393.

Sherrod, B. L., R. J. Blakely, C. S. Weaver, H. M. Kelsey, E. Barnett, L. M. Liberty, K. L. Meagher, and K. M. Pape (2008). Finding concealed active faults: extending the southern Whidbey Island fault across the Puget lowland, Washington, *J. Geophys. Res.*, **113,** B05313, doi 10.1029/2007JB005060.

Snelson, C. M., T. M. Brocher, K. C. Miller, T. L. Pratt, and A. M. Tréhu (2007). Seismic amplification within the Seattle basin, Washington State: insights from SHIPS seismic tomography experiments, *Bull. Seismol. Soc. Am.* **97,** no. 5, 1432–1448 doi 10.1785/0120050204.

Suppe, J., and D. A. Medwedeff (1990). Geometry and kinematics of fault-propagation folding, *Ecol. Geol. Helv.* **83,** 409–454.

ten Brink, U. S., J. Song, and R.C. Bucknam (2006). Rupture models for the A.D. 900–930 Seattle fault earthquake from uplifted shorelines, *Geology* **34,** 585–588, doi 10.1130/G22173.1.

ten Brink, U. S., P. C. Molzer, M. A. Fisher, R. J. Blakely, R. C. Bucknam, T. Parsons, R. S. Crosson, and K. C. Creager (2002). Subsurface geometry and evolution of the SFZ and the Seattle basin, Washington, *Bull. Seismol. Soc. Am.* **92,** 1737–1753.

Van Wagoner, T. M., R. S. Crosson, K. C. Creager, G. F. Medema, L. A. Preston, N. P. Symons, and T. M. Brocher (2002). Crustal structure and relocated earthquakes in the Puget Lowland, Washington from high resolution seismic tomography, *J. Geophys. Res.* **107,** no. B12, 2381, doi 10.1029/2001JB000710.

Walsh, T. J. (1983). Map of coal mine workings in part of King County, Washington, *Wash. Div. Geol. Earth Res. Open-File Rept. OF 83-17*, 4 pp., scale 1:24000.

Walsh, T. J. (1984). Geology and coal resources of central King County, Washington, *Wash. Div. Geol. Earth Res. Open-File Rept. OF 84-3*, 24 pp.

Wells, R. E., C. S. Weaver, and R. J. Blakely (1998). Fore-arc migration in Cascadia and its neotectonic significance, *Geology* **26,** 759–762.

Yilmaz, O. (2001). *Seismic Data Analysis: Processing, Inversion, and Interpretation of Seismic Data*, Society of Exploration Geophysicists, Tulsa, Oklahoma, 2027 pp.

Yount, J. C., and H. D. Gower (1991). Bedrock geologic map of the Seattle 300 by 600 quadrangle, Washington, *U.S. Geol. Surv. Open-File Rept. 91–147*, scale 1:100,000, 37 pp., 4 plates.

Center for Geophysical Investigation of the Shallow Subsurface (CGISS)
Boise State University
1910 University Drive
Boise, Idaho 83725-1536
lliberty@boisestate.edu
(L.M.L.)

U.S. Geological Survey
School of Oceanography
Box 357940
University of Washington
Seattle, Washington 98195
tpratt@ocean.washington.edu
(T.L.P.)

Manuscript received 12 June 2007